

Zero Energy Modes and Statistics of Vortices in Spinful Chiral p -Wave Superfluids

Takuto KAWAKAMI*, Takeshi MIZUSHIMA, and Kazushige MACHIDA

Department of Physics, Okayama University, Okayama 700-8530

Possible stable singular vortex (SV) and half-quantum vortex (HQV) of superfluid $^3\text{He-A}$ phase confined in restricted geometries are investigated. The associated low energy excitations are calculated in connection with possible existence of Majorana zero modes obeying non-Abelian statistics. The energetics between those vortices are carefully examined by using the standard Ginzburg-Landau functional with the strong coupling correction. The Fermi liquid effect, which is not included there, is considered approximately within the London approach. This allows us to determine the stability regions in pressure, temperature, and applied field for SV and HQV. The existence of Majorana zero mode and its statistics, either Abelian or non-Abelian under braiding of SVs are studied by solving Bogoliubov-de Gennes equation for this spinful chiral p -wave superfluids. We determine several conditions for controllable external parameters, pressure, field direction and strength for non-Abelian statistics of Majorana zero modes to realize.

KEYWORDS: chiral p -wave superfluids, vortex, zero energy state, non-Abelian statistics, Ginzburg-Landau theory, Bogoliubov-de Gennes equation

1. Introduction

Much attention has been paid on various exotic vortices and the associated low energy excitations in spin-triplet p -wave superfluids and superconductors.¹⁻³⁾ In particular, there is a considerable amount of investigations for the quasiparticle whose energy eigenvalue is exactly zero and creation and annihilation operators are the self-Hermitian: $\gamma_{E=0} = \gamma_{E=0}^\dagger$.^{4,5)} Fermionic field operators that have self-Hermitian creation and annihilation operators are called the Majorana fermions⁶⁾ and the quasiparticle energy modes with $\gamma_{E=0} = \gamma_{E=0}^\dagger$ are called the Majorana zero energy states (ZES). The Majorana ZESs localized at vortices are thought to be useful for fault-tolerant quantum computations because they can obey the non-Abelian statistics.^{5,7-10)}

The localized Majorana ZESs have been pointed out in the quasi-hole of the Pfaffian state of the quantum Hall state with the $5/2$ filling.^{4,5)} The other candidate systems that support Majorana ZESs are quantized vortices in chiral p -wave superfluids or superconductors,^{7,11-17)} the surface Andreev bound state of chiral or time reversal symmetric p -wave superfluids,¹⁸⁻²³⁾ the junction between an s -wave superconductor and a topological insulator,²⁴⁻²⁷⁾ and the s -wave superfluid with particular spin-orbit interactions.²⁸⁾

First of all, we consider Majorana ZESs bound at a singular vortex in spin polarized p -wave superfluids, which involves the particle-hole symmetry $\gamma_E = \gamma_{-E}^\dagger$. Then the existence of the exact ZES is guaranteed by the index theorem²⁹⁾ and the analytic solution of the Caroli-de Gennes-Matricon state when the vorticity is odd.^{12,17,30,31)} Therefore the existence of the Majorana ZES is topologically protected. The eigenstates of the system constructed by Majorana quasiparticles are described by the occupation of the complex fermion state, that is, the linear combination of the two Majorana

quasiparticles $c_{2j} = (\gamma_{2j} + i\gamma_{2j+1})/\sqrt{2}$. For spin polarized systems, the complex fermion is formed by a pair of the Majorana ZESs γ_j and γ_{j+1} in between spatially separated vortices, giving rise to the non-locality of the complex fermion. If an well-isolated vortex has an odd number of the Majorana ZESs, the complex fermion state is necessarily constructed by the spatially separated Majorana ZES and the vortices obey the non-Abelian statistics because of the non-locality of their excitations.⁷⁾ For the system where the spin-degrees of freedom, for example the spin $|\uparrow\uparrow\rangle$ and $|\downarrow\downarrow\rangle$ pairs, survives, an isolated singular vortex (SV) has degeneracy of the ZESs in two spin sectors.³²⁾ The statistics of the SV in spinful superfluids depends on the ways to form the complex fermion as follows. If the two Majorana quasiparticles constructing a complex fermion eigenstate are in the single vortex core, the statistics is Abelian. If they are in spatially separated vortices, however, the statistics is non-Abelian. Thus the half-quantum vortex (HQV) that has the singularity in either the spin $|\uparrow\uparrow\rangle$ or $|\downarrow\downarrow\rangle$ component of the order parameter is more capable for the non-Abelian statistics.⁷⁾

The superfluid $^3\text{He-A}$ phase is one of the most useful candidate of the p -wave superfluid associated with the Majorana ZES in the sense that the ground states are most established^{1,33)} and there are many experiments and samples with controllable parameters.³⁴⁻³⁸⁾ Since the superfluid $^3\text{He-A}$ phase is a spinful system, the statistics of the vortex in spinful p -wave superfluids should be clarified.

In order to observe the Majorana character, it is necessary to set up a two dimensional system where the thickness of the sample is much shorter than the dipole coherence length. The possible experiment has been set up by Saunders group, where they confine superfluid ^3He in the slab geometry whose thickness is $0.6\ \mu\text{m}$ under the following conditions: The pressures are between 0 and 5.5 bar, the temperature is cooled to $350\ \mu\text{K}$, and the external field is applied to perpendicular to the slab for car-

*E-mail address: kawakami@mp.okayama-u.ac.jp

rying out the NMR observation. Then they observe the phase transition from the A-phase to the unknown phase under low pressure and temperature region. Investigation of vortices in spinful chiral p -wave superfluids and their features also leads us to understand such a character of $^3\text{He-A}$ in the slab in future.

For rotating experiments, Yamashita *et al.*³⁶⁾ have recently performed an experiment in parallel plate geometry intended to observe the HQV in superfluid $^3\text{He-A}$. The superfluid is confined in a cylindrical region with the radius $R = 1.5$ mm and the height 12.5 μm sandwiched by parallel plates. A magnetic field $H = 26.7$ mT ($\parallel \mathbf{z}$) is applied perpendicular to the parallel plates, and a pressure is $P = 3.05$ MPa. In this pressure, the strong coupling effect due to the spin fluctuations becomes important.³⁹⁾ Since the gap 12.5 μm between plates is narrow compared to the dipole coherence length $\xi_d \sim 10$ μm , the l -vectors, which signifies the direction of orbital angular momentum of Cooper pairs, are always perpendicular to the plates. Also the d -vectors are confined within the plane by an applied field $\mathbf{H} \parallel \mathbf{z}$ because the dipole magnetic field is $H_d \sim 2.0$ mT,¹⁾ where H tends to align the d -vectors perpendicular to the field direction. Yamashita *et al.* investigate to seek out various parameter spaces, such as temperature T , or the rotation speed Ω up to $\Omega = 6.28$ rad/s by using the rotating cryostat in ISSP, Univ. of Tokyo, capable for the maximum rotation speed ~ 12 rad/s, but there is no evidence for the HQV.³⁶⁾

The stability of HQVs has been argued since they were pointed out by Volovik and Mineev.⁴⁰⁾ The hydrodynamical calculation taking account of the Fermi liquid (FL) correction shows that the HQV is energetically stable against the SV.^{2, 41–44)} However, in the previous paper,⁴⁵⁾ we have carried out the calculation based on the full Ginzburg-Landau (GL) theory taking account of the strong coupling correction due to the spin fluctuations, which plays an crucial role for the stability of the A-phase at high pressure, without the FL correction. This implies that the HQV is unstable unless the pairing phase becomes the so-called A_2 phase under strong external field.⁴⁵⁾ In this paper, we find that the contributions from the strong coupling and the FL corrections are competitive on the stability of the HQV at realistic rotation speed and high pressure in the experiment using rotating cryostat in ISSP. Therefore, in order to clarify the statistics of vortices in the spinful p -wave superfluid, we have to examine the statistics of the SV, in addition to that of the HQV on an equal footing.

This paper is arranged as follows: In §2, we derive the spinful Bogoliubov-de Gennes (BdG) equation and introduce the GL free energy. In §3, we discuss the energetics of the vortex textures and the stability of the HQV. We calculate the energetically advantage of the HQV originating from the FL correction and disadvantage from the spin-fluctuation strong coupling correction using both the London limit calculation and full GL calculation. In §4, we examine the statistics of the SV using numerical calculation of the spinful BdG equation. In §4.1, we discuss the case where the direction of d -vectors is perpendicular to the external field. In this section, we clarify that when the vortex distance is finite, two eigenstates

originating from ZESs in the different spin sectors do not hybridize with each other so that the braiding of the SV does not commute necessarily. In §4.2, we consider the case where the direction of d -vectors is tilted from the direction perpendicular to the external field. In this situation, we demonstrate that the Zeeman effect due to an external field parallel to the d -vectors hybridizes the two Majorana ZESs. In final section, we present our summary and conclusions.

2. Formulation

2.1 Spinful Bogoliubov-de Gennes equation

In general the OPs for spin triplet superfluids are described as

$$\hat{\Delta}(\mathbf{r}_1, \mathbf{r}_2) \equiv \begin{bmatrix} \Delta_{\uparrow\uparrow}(\mathbf{r}_1, \mathbf{r}_2) & \Delta_{\uparrow\downarrow}(\mathbf{r}_1, \mathbf{r}_2) \\ \Delta_{\downarrow\uparrow}(\mathbf{r}_1, \mathbf{r}_2) & \Delta_{\downarrow\downarrow}(\mathbf{r}_1, \mathbf{r}_2) \end{bmatrix}, \quad (1)$$

where $\Delta_{\sigma\sigma'} = -V(\mathbf{r}_1, \mathbf{r}_2) \langle \psi_\sigma(\mathbf{r}_1) \psi_{\sigma'}(\mathbf{r}_2) \rangle$ and $\psi_\sigma(\mathbf{r})$ is the field operator of fermions with spin $\sigma = \uparrow, \downarrow$. The spinful mean-field Hamiltonian of the spin-triplet superfluids and superconductors is described by using this notation as

$$\mathcal{H} = E_0 + \frac{1}{2} \int d\mathbf{r}_1 \int d\mathbf{r}_2 \Psi^\dagger(\mathbf{r}_1) \underline{\mathcal{K}}(\mathbf{r}_1, \mathbf{r}_2) \Psi(\mathbf{r}_2), \quad (2)$$

$$\Psi(\mathbf{r}) = [\psi_\uparrow(\mathbf{r}), \psi_\downarrow(\mathbf{r}), \psi_\uparrow^\dagger(\mathbf{r}), \psi_\downarrow^\dagger(\mathbf{r})]^T, \quad (3)$$

$$\underline{\mathcal{K}}(\mathbf{r}_1, \mathbf{r}_2) = \begin{bmatrix} \hat{H}_0(\mathbf{r}_1, \mathbf{r}_2) & \hat{\Delta}(\mathbf{r}_1, \mathbf{r}_2) \\ -\hat{\Delta}^*(\mathbf{r}_1, \mathbf{r}_2) & -\hat{H}_0^*(\mathbf{r}_1, \mathbf{r}_2) \end{bmatrix}, \quad (4)$$

$$\hat{H}_0(\mathbf{r}_1, \mathbf{r}_2) = \delta(\mathbf{r}_1 - \mathbf{r}_2) [H_0(\mathbf{r}_1) \hat{1} + \mu_n \mathbf{H} \cdot \hat{\boldsymbol{\sigma}}]. \quad (5)$$

where $\Psi(\mathbf{r})$ is the spinor in the Nambu space, $\hat{1}$ is a 2×2 unit matrix, and μ_n , \mathbf{H} , and $\hat{\boldsymbol{\sigma}}$ are the magnetic moment of ^3He atoms, the external field, and the 2×2 Pauli matrices respectively. Here, we assume that the superfluids and superconductors are confined by the potential with magnitude $V_0 \gg |\Delta_{\sigma\sigma'}|$. Then the single particle part $H_0(\mathbf{r})$ are given as

$$H_0(\mathbf{r}) = -\frac{\nabla^2}{2M} + V_0 \theta(r - R) - \mu + i\Omega \cdot (\mathbf{r} \times \nabla), \quad (6)$$

where M , μ , and Ω are the mass of the particle, the chemical potential, and the external rotation respectively. We set $\hbar = 1$.

In general, the OP of p -wave superfluids is expanded in terms of the eigenstates of the orbital angular momentum of the Cooper pair $l_z = -1, 0, 1$. We assume the system to be spinful chiral p -wave superfluids, namely, the orbital ferromagnetic state so that the only $l_z = -1$ component survives. This can be realized in parallel plate geometry and slab, where the dipole coherence length is much longer than the thickness of the sample. Then the explicit expression of the OPs is given as

$$\Delta_{\sigma\sigma'} \left(\frac{\mathbf{r}_1 + \mathbf{r}_2}{2}, \tilde{\mathbf{k}} \right) = -A_{\sigma\sigma', -1} \left(\frac{\mathbf{r}_1 + \mathbf{r}_2}{2} \right) \times \frac{\tilde{k}_x - i\tilde{k}_y}{k_F} \exp[-(\tilde{k}^2 - k_F^2) \xi_p^2], \quad (7)$$

where $\tilde{\mathbf{k}}$ is the relative momentum and ξ_p is the size of the Cooper pair. The components in eq. (1) are obtained

as the Foulrier transformation of eq. (7) with respect to the relative coordinate

$$\Delta_{\sigma\sigma'}(\mathbf{r}_1, \mathbf{r}_2) = -A_{\sigma\sigma',-1} \left(\frac{\mathbf{r}_1 + \mathbf{r}_2}{2} \right) \times \frac{ix_{12} + y_{12}}{8\pi\xi_p^4 k_F} \exp \left[-\frac{r_{12}^2}{4\xi_p^2} + k_F^2 \xi_p^2 \right], \quad (8)$$

where k_F is the fermi wave number.

We carry out the Bogoliubov transformation from the fermionic field operator to the quasiparticle basis with $\Gamma_\nu = [\Gamma_{\nu\uparrow}, \Gamma_{\nu\downarrow}, \Gamma_{\nu\uparrow}^\dagger, \Gamma_{\nu\downarrow}^\dagger]^T$ in the Nambu space,

$$\Psi(\mathbf{r}) = \sum_\nu \underline{u}_\nu(\mathbf{r}) \Gamma_\nu,$$

$$\underline{u}_\nu(\mathbf{r}) = [\mathbf{u}_\nu^{(1)}, \mathbf{u}_\nu^{(2)}, \{\mathcal{T}_1 \mathbf{u}_\nu^{(1)}\}^*, \{\mathcal{T}_1 \mathbf{u}_\nu^{(2)}\}^*],$$

where \mathcal{T}_i is the 4×4 matrix defined with Pauli matrix. The transformation matrix $\underline{u}_\nu(\mathbf{r})$ must satisfy the orthonormality $\int d\mathbf{r}_1 \underline{u}_\nu^\dagger(\mathbf{r}_1) \underline{u}_\mu(\mathbf{r}_1) = \delta_{\nu,\mu} \mathbf{1}$ and the completeness $\sum_\nu d\mathbf{r}_1 \underline{u}_\nu(\mathbf{r}_1) \underline{u}_\nu^\dagger(\mathbf{r}_2) = \delta(\mathbf{r}_1 - \mathbf{r}_2) \mathbf{1}$ where $\mathbf{1} = \text{diag}(\hat{1}, \hat{1})$ is a 4×4 unit matrix. In order to obtain the operators of the quasiparticles that diagonalize the mean field Hamiltonian eq. (2) as

$$\mathcal{H} = E_0 + \frac{1}{2} \Gamma_\nu^\dagger E_\nu \Gamma_\nu, \quad (9)$$

$$E_\nu \equiv \text{diag} \left(E_\nu^{(\uparrow)}, E_\nu^{(\downarrow)}, -E_\nu^{(\uparrow)}, -E_\nu^{(\downarrow)} \right), \quad (10)$$

one can find that the wave functions of the quasiparticles $\mathbf{u}_\nu^{(1)}(\mathbf{r})$ and $\mathbf{u}_\nu^{(2)}(\mathbf{r})$ should obey the same BdG equation described as

$$\int d\mathbf{r}' \underline{K}(\mathbf{r}, \mathbf{r}') \mathbf{u}_\nu(\mathbf{r}') = E_\nu^\sigma \mathbf{u}_\nu(\mathbf{r}), \quad (11)$$

$$\mathbf{u}_\nu(\mathbf{r}) = [u_\nu^\uparrow(\mathbf{r}), u_\nu^\downarrow(\mathbf{r}), v_\nu^\uparrow(\mathbf{r}), v_\nu^\downarrow(\mathbf{r})]. \quad (12)$$

Then the annihilation operator of the quasiparticle is expressed as

$$\Gamma_{\nu\sigma} = \int d\mathbf{r} \{ \mathbf{u}_\nu(\mathbf{r}) \}^\dagger \Psi(\mathbf{r}). \quad (13)$$

We numerically diagonalize the BdG equation (11) under the gap potential given in eq. (7) with

$$A_{\sigma\sigma',-1}(\mathbf{r}) = A_{\sigma\sigma',-1}^0 \prod_{j=1}^{N_v} \exp[i\kappa_j \theta_j] \tanh \left(\frac{r_j}{\xi_{\sigma\sigma'}} \right), \quad (14)$$

where κ_j is the winding number of the component in the j -th vortex, θ_j and r_j is the azimuthal angle and radius centered by j th vortex, and $\xi_{\sigma\sigma'}$ is the coherence length of the OP in the spin sector $|\sigma\sigma'\rangle$. We assume the uniformity of the OPs along the z direction. For the quasiparticle eigenstate in the BdG equation (11), we impose the periodic boundary condition with the wave number k_z , that is, $\mathbf{u}_\nu = \mathbf{u}_{E,k_z}(x, y) \exp[ik_z z]$ and $\Gamma_{\nu\sigma} = \Gamma_{E,k_z,\sigma}$. Then the BdG equation (11) is block-diagonalized in terms of k_z . In the subspace, the particle-hole symmetry $\{\mathcal{T}_x \underline{K} \mathcal{T}_x\}^* = -\underline{K}$ gives $\hat{\mathcal{T}}_x \{ \mathbf{u}_{E,k_z} \exp[ik_z z] \}^* = \mathbf{u}_{-E,k_z} \exp[ik_z z]$ and inversion symmetry along the z direction gives $\mathbf{u}_{E,k_z} = \mathbf{u}_{E,-k_z}$ and $E(-k_z) = E(k_z)$. Thus one finds $\Gamma_{E,k_z,\sigma}^\dagger = \Gamma_{-E,-k_z,\sigma}$, which implies that the quasiparticle arising from $k_z = 0$ can be the Majorana

zero mode $\Gamma_{0,0,\sigma} = \Gamma_{0,0,\sigma}^\dagger = \gamma^\sigma$. We focus on the eigenstate with $k_z = 0$ throughout this work. The numerical diagonalization is carried out by the discrete variable representation method.^{46–49}

2.2 Ginzburg-Landau framework

We use the GL framework to discuss the stable textures and the energetics of the vortex, which is quantitatively reliable for ^3He . Then we assume that the OPs are decomposed to the center-of-mass coordinate and the orbital degrees of freedom with the relative momentum around $|k| \simeq k_F$. These components are described with the 3×3 matrix $A_{\mu i} = A_{\mu i}(\mathbf{r})$ as

$$\hat{\Delta}(\mathbf{r}, \hat{\mathbf{k}}) = \begin{bmatrix} -A_{xi} + iA_{yi} & \sqrt{2}A_{zi} \\ \sqrt{2}A_{zi} & A_{xi} + iA_{yi} \end{bmatrix} \hat{k}_i \quad (15)$$

$$= \begin{bmatrix} A_{\uparrow\uparrow m} & A_{\uparrow\downarrow m} \\ A_{\uparrow\downarrow m} & A_{\downarrow\downarrow m} \end{bmatrix} \hat{k}_m, \quad (16)$$

where $i = x, y, z$, $m = -1, 0, +1$, $\hat{k}_\pm = (\hat{k}_x \mp i\hat{k}_y)\sqrt{2}$, and $\hat{\mathbf{k}}$ is the unit vector oriented to the direction of the momentum on the Fermi surface. The GL free energy functional which is invariant under gauge transformation, and spin and orbital space rotation is well-established^{1, 2, 33–35, 50–53} and given by the standard form

$$f_{\text{total}} = f_{\text{bulk}}^{(2)} + f_{\text{bulk}}^{(4)} + f_{\text{grad}} + f_{\text{dipole}} + f_{\text{field}}, \quad (17)$$

$$f_{\text{bulk}}^{(2)} = -\alpha A_{\mu i}^* A_{\mu i}, \quad (18)$$

$$f_{\text{bulk}}^{(4)} = \beta_1 A_{\mu i}^* A_{\mu i}^* A_{\nu j} A_{\nu j} + \beta_2 A_{\mu i}^* A_{\nu j}^* A_{\mu i} A_{\nu j} + \beta_3 A_{\mu i}^* A_{\nu i}^* A_{\mu j} A_{\nu j} + \beta_4 A_{\mu i}^* A_{\nu j}^* A_{\mu j} A_{\nu i} + \beta_5 A_{\mu i}^* A_{\mu j}^* A_{\nu i} A_{\nu j}, \quad (19)$$

$$f_{\text{grad}} = K_1 (\partial_i^* A_{\mu j}^*) (\partial_i A_{\mu j}) + K_2 (\partial_i^* A_{\mu j}^*) (\partial_j A_{\mu i}) + K_3 (\partial_i^* A_{\mu i}^*) (\partial_j A_{\mu i}), \quad (20)$$

$$f_{\text{dipole}} = g_d (A_{\mu\mu}^* A_{\nu\nu} + A_{\mu\nu}^* A_{\nu\mu} - \frac{2}{3} A_{\mu\nu}^* A_{\mu\nu}). \quad (21)$$

$$f_{\text{field}} = g_m H_\mu A_{\mu i}^* H_\nu A_{\nu i}, \quad (22)$$

In the weak coupling limit, the GL parameters and coupling constant of the dipole energy⁵² are

$$\alpha = \alpha_0 (1 - T/T_c), \quad \alpha_0 = \frac{N(0)}{3},$$

$$\beta_2^W = \beta_3^W = \beta_4^W = -\beta_5^W = -2\beta_1^W$$

$$= 2\beta_0^W = \frac{7\zeta(3)N(0)}{120(\pi k_B T_c)^2},$$

$$K_1 = K_2 = K_3 = \frac{7\zeta(3)N(0)(\hbar v_F)^2}{240(\pi k_B T_c)^2},$$

$$g_d = \frac{\mu_0}{40} \left[\gamma \hbar N(0) \ln \frac{1.1339 \times 0.45 T_F}{T_c} \right],$$

$$g_m = \frac{7\zeta(3)N(0)(\gamma \hbar)^2}{48[(1+F_0^a)\pi k_B T_c]}.$$

The details of the physical constants in the form described above are as follows: The transition temperature T_c , the density of states $N(0)$, the Fermi velocity v_F , the permeability of vacuum μ_0 , the gyromagnetic ratio γ , and Fermi temperature T_F . These are given by the experiments^{34, 35} and depend on the pressure. In the high pressure region, the GL parameters of the bulk 4th or-

der terms β_i are corrected by the strong coupling effect due to the spin fluctuations. For β_i , we use the strong coupling correction calculated by Sauls and Serene,⁵⁰⁾ as mentioned below.

3. Energetics of Vortex Textures

Without loss of generality, we use the description for the OP $A_{\mu i} = d_{\mu} A_i$, where the d -vector d_{μ} and A_i are complex values. For the bulk of the ^3He -A phase, the d -vectors can be a unit vector, but we consider the generic situation on d -vectors throughout this work. First, let us define textures under the situation that all the d -vectors lie in the x - y plane. This situation is approximately realized in ^3He between parallel plates under the strong field $H \gg H_d$. If we choose the direction perpendicular to the plane as the spin quantization axis, then $A_{\uparrow\downarrow, m} = 0$. In this case, we can find the following two possibilities on the vortex textures. One of them is the HQV: At the vortex core, either $A_{\uparrow\uparrow, m}$ or $A_{\downarrow\downarrow, m}$ component of the OP has an unit winding number and singularity. The other is the SV: The singularities of both the spin components of OPs are in the same position.

In the zero-field case, the single SV has two zero energy modes originating from the spin $|\uparrow\uparrow\rangle$ and $|\downarrow\downarrow\rangle$ sectors, whereas the HQV has a single zero energy mode from the spin sector which has the phase singularity in the OP. The low energy bound state at the vortex core of the HQV is same as that of the singular vortex in spinless chiral p -wave superfluids. Therefore it is well-known that HQVs obey the non-Abelian statistics.⁷⁾

However, the energetics of the HQV against the SV still remains as a problem. Specifically, for the realistic set of the GL parameters in ^3He , the FL correction maintains the stability of the HQV. In contrast, it is demonstrated here that the strong coupling effect on the bulk 4th order terms that stabilizes the A-phase against the B-phase is not favorable for the stability of the HQV. Based on the GL theory, we examine here the stability of the HQV as a consequence of the competition between the strong-coupling effect and the FL correction.

The strong coupling effect in the bulk 4th order term is derived by Anderson and Brinkman³⁹⁾ as

$$\begin{aligned} \beta_1 &= -(1 + 0.1\delta)\beta_0^W, & \beta_2 &= (2 + 0.2\delta)\beta_0^W, \\ \beta_3 &= (2 - 0.05\delta)\beta_0^W, & \beta_4 &= (2 - 0.55\delta)\beta_0^W, \\ \beta_5 &= -(2 + 0.7\delta)\beta_0^W, \end{aligned} \quad (23)$$

where δ is the spin-fluctuation parameter depending on the pressure.³³⁾ Thus the bulk 4th order terms of the GL free energy in eq. (19) are

$$f_{\text{bulk}}^{(4)} = B_d(|d_{\uparrow\uparrow}|^4 + |d_{\downarrow\downarrow}|^4) + B_c(|d_{\uparrow\uparrow}|^2|d_{\downarrow\downarrow}|^2), \quad (24)$$

where

$$\begin{aligned} B_d &= \beta_0^W [(4 - 0.35\delta)(|A_{+1}|^4 + |A_{-1}|^4) \\ &\quad + (16 - 0.55\delta)|A_{+1}|^2|A_{-1}|^2], \end{aligned} \quad (25)$$

$$\begin{aligned} B_c &= -\beta_0^W \delta [3.5(|A_{+1}|^4 + |A_{-1}|^4) \\ &\quad + 9|A_{+1}|^2|A_{-1}|^2] < 0, \end{aligned} \quad (26)$$

where $A_m = (A_x - \text{sgn}(m)iA_y)/\sqrt{2}$, $d_{\sigma\sigma} = (d_x - \text{sgn}(\sigma)id_y)/\sqrt{2}$, and $d_{\uparrow\downarrow} = d_z$. If both the spin $|\uparrow\uparrow\rangle$ and $|\downarrow\downarrow\rangle$ components of the OP remain finite, the free energy decreases with increasing δ because $B_c < 0$ in eq. (24). The amplitude of the OP in both the spin sectors is enhanced by each other through the strong coupling effect. In the case of the core of the HQV, one of the spin component must have the singularity so that another component is not enhanced by the mechanism arising from $B_c < 0$.

In order to quantify the strong coupling effect, we carry out the numerical minimization of the GL free energy in eq. (17) composed of the bulk, gradient, and dipole energy in eqs. (18), (19), (20), and (21). Our numerical condition is as follows. We assume that the l -vectors align to the z direction and the d -vectors are in xy plane. The uniformity of the OPs is also assumed along the z direction so that the spin and orbital indices of OPs $A_{\mu i}$ reduce to $\mu, i = x, y$ and our calculation is carried out in a 2D plane. Then the magnetic interaction energy in eq. (22) can be ignored. This situation can be realized in the parallel plate geometry^{36, 37)} where the distance between the parallel plates is shorter than the dipole coherence length ($\sim 10 \mu\text{m}$) and much longer than the coherence length ($\sim 10 \text{nm}$). Here, we impose the rigid boundary condition with the radius R on the OPs as $A_{\mu i}(|\mathbf{r}| = R) = 0$. We use the GL parameters β_i in eq. (19) taking account of the strong coupling correction given by Sauls and Serene,⁵⁰⁾ and their values are qualitatively consistent with eq. (23). In Fig. 1, we show the amplitudes of dominant components $A_{\uparrow\uparrow, +1}$ and $A_{\downarrow\downarrow, +1}$ for the SV and the HQV. In order to compare these energies in equal footing, we set up two singular vortices for the SV texture and four half-quantum vortices for the HQV texture. In our calculation, however, the HQV texture is only the saddle-point solution of GL equation since the HQV can be continuously transformed into SV texture and the free energy of the HQV is always higher than that of the SV as long as the FL correction is neglected.

In refs. 42, 43, and 44, the OPs in the HQV are restricted within the bulk A-phase. The strong coupling effect equally affects the free energy of both the HQV and SV texture under this assumption. In our work, we investigate the energetics of the vortices without the restriction even at the vortex core and take account of the strong coupling effect. Then the strong coupling effect near the vortex core gives the HQV relative energetically disadvantage compared with the SV as shown below.

We analyze the energetics between these two textures in details. In Fig. 2, we show the difference of the bulk and gradient energies of the HQV from the SV, normalized with $K|\Delta|^2$ as a function of the pressure. The features of the HQV texture result from two factors: (i) As seen in Fig. 1(c), the amplitude of the component $A_{\downarrow\downarrow, +1}$ is depressed at the singularity of $A_{\uparrow\uparrow, +1}$. (ii) Near the singularity, the component $A_{\uparrow\uparrow, +1}$ in the HQV is more enhanced than that of the SV as seen in the upper panel of Fig. 1(c), because the bulk 4th order term with $B_c < 0$ in eq. (26) gets the interaction between $A_{\uparrow\uparrow, m}$ and $A_{\downarrow\downarrow, m}$ attractive. The bulk energy of $|\downarrow\downarrow\rangle$ component is increased

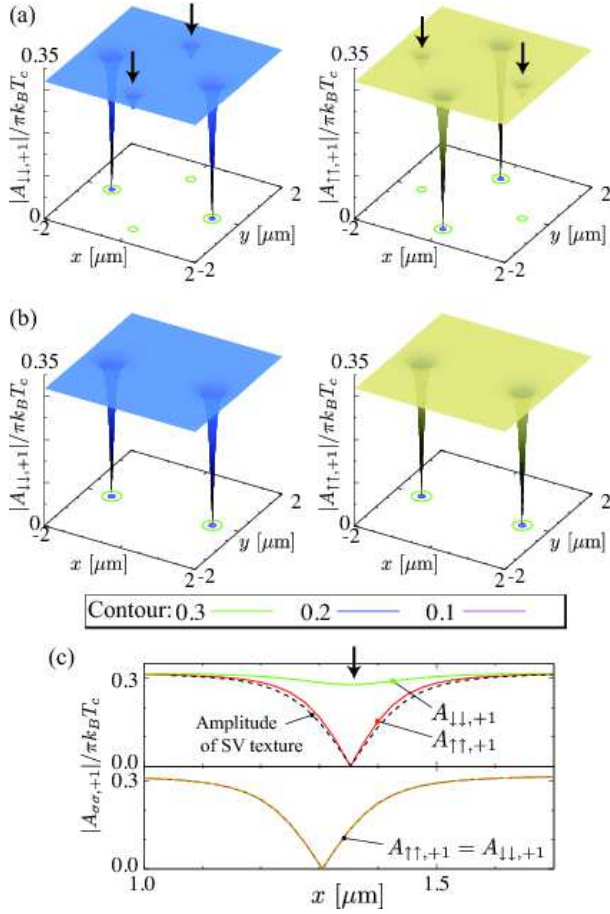


Fig. 1. (Color online) Spatial profiles of the dominant component $|A_{\sigma\sigma,+1}|$ for the four-HQVs (a) and the two-SVs (b) textures near the center of the system, and (c) their cross section magnifying the vortex core region. The upper (lower) panel in (c) is the spatial profile of the HQV (SV). The non-singular component of the HQV is depressed at the vortex core signified with the arrow in (a) and (c). The broken line in upper panel of (c) is the amplitude of $|A_{\sigma\sigma,+1}|$ of the SV when the position of the vortex core coincides with that of the HQV. In all the figures, the system size is set to be $R = 5 \mu\text{m}$, the rotating speed is $\Omega = 3 \times 10^3 \text{ rad/s}$, and temperature $T = 0.95T_c$, where the SV is the energetically stable. The unit of the x and y axis is micrometer and the amplitudes of the OPs are normalized with $\pi k_B T_c$.

by the factor (i) and that of the spin $|\uparrow\uparrow\rangle$ component lowers due to the factor (ii). As seen in Fig. 2, the bulk energies of the HQV relative to the SV is the negative in high pressure region and as the pressure becomes lower, that is, the strong coupling correction becomes less important, the bulk energy of the HQV is eventually higher than that of SV. This result implies that the bulk energy with the strong coupling correction favors the HQV.

However, the gradient energy of the HQV is considerably larger than that of the SV at the vortex cores. As seen in the Fig. 2, the gradient energy of the HQV relative to the SV becomes larger than that of the bulk energy, so that the HQV is not stable in this consideration without the FL correction. The reason of this disadvantage of the gradient energy for the stability of the HQV is as follows. By the factor (i), that is, the depression of the OP without the vortex singularity at the vortex core of the HQV seen in Fig. 1, the loss of the

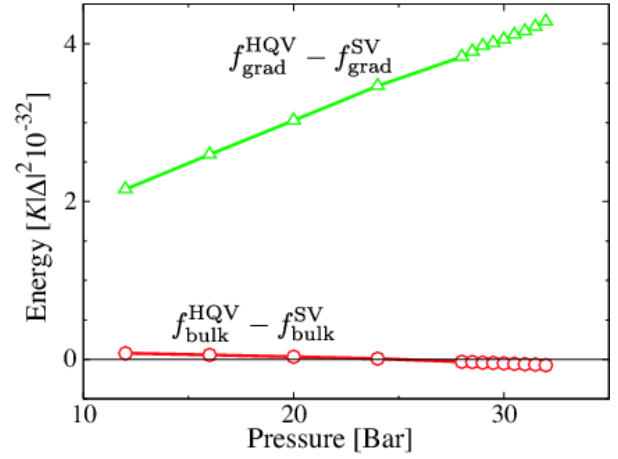


Fig. 2. (Color online) Difference of the gradient and bulk energies of the HQV from that of the SV normalized with $K|\Delta|^2$ as a function of the pressure.

energy appears due to the spatial modulation. Furthermore, the kinetic energy due to the phase winding is also enhanced by the fact that the singular component $A_{\uparrow\uparrow,+1}$ is enhanced by the factor (ii). The strong coupling effect plays a crucial role on the stability of the HQV in the high pressure regime, while this becomes less important in the low pressure regime so that these disadvantages due to the gradient energy may be negligible.

Although the FL correction is the key factor for the stability of the HQV,^{42–44} it is difficult to take account of these effects into our calculation based on the GL framework using more generic form of OPs. In order to discuss the FL correction, we apply the London approximation to the OPs, where $A_{+1}(\mathbf{r}) = |\Delta_A| \exp[i\Phi(\mathbf{r})]$, $A_{-1}(\mathbf{r}) = 0$, and the d -vector is assumed as the unit vector $[d_x, d_y, d_z] = [\cos \alpha(\mathbf{r}), \sin \alpha(\mathbf{r}), 0]$. We can treat the FL correction as the effective mass of the spin current by using this representation. Note that this representation restricts the pairing phase to the A-phase so that we can not describe the vortex core and boundary of the system exactly. The FL correction makes the mass of the spin current lighter than that of the mass current, that is, $\rho_{\text{sp}}/\rho_s < 1$ where ρ_{sp} and ρ_s are the effective mass of the spin and mass current respectively.

The gradient term with the FL correction is described with the London approximation as^{33,42)}

$$\frac{f_{\text{grad}}}{2K|\Delta_A|^2 \rho_s / \rho_s^0} = (\nabla \Phi + \mathbf{r} \times \Omega)^2 + (\rho_{\text{sp}}/\rho_s) (\nabla \alpha)^2. \quad (27)$$

If we consider an axially symmetric vortex, $\Phi = q^s \phi$, $\alpha = q^{\text{sp}} \phi$, where ϕ is the azimuthal angle of the system centered in the vortex singularity and q^s and q^{sp} are the mass and spin circulation. The HQV texture has the circulation $(q^s, q^{\text{sp}}) = (1/2, 1/2)$, whereas the SV has $(q^s, q^{\text{sp}}) = (1, 0)$. Thus the spatial variation term of the GL free energy for each texture is

$$\int d\mathbf{r} \frac{f_{\text{grad}}}{2\pi K|\Delta_A|^2 \rho_s / \rho_s^0}$$

$$= \begin{cases} \frac{1}{2} \left(1 + \frac{\rho_{sp}}{\rho_s} \right) \ln \left(\frac{R}{\xi_{\sigma\sigma}} \right) & (\text{HQV}) \\ \ln \left(\frac{R}{\xi_{\sigma\sigma}} \right) & (\text{SV}) \end{cases} \quad (28)$$

where the energy of the HQV texture is twice larger than that of the single axially symmetric HQV and we set the external rotation to be $\Omega = 0$. For $\rho_{sp} = \rho_s$, the energy of the HQV arising from the spatial variation of the OPs is equivalent to that of the SV. If ρ_{sp} is smaller than ρ_s due to the FL correction, the energetically advantage of the HQV texture increases logarithmically as system size R becomes large.

We numerically estimate this effect in the London limit which neglects the vortex core under the same conditions as our full GL calculation, such as the geometry and the vortex configuration. From the GL calculation, we find that the amplitude of OPs recovers to the bulk within about $0.5 \mu\text{m}$ from the vortex core as shown in Fig. 1. Then we neglect this region from contribution and calculate the spatial variation energy based on eq. (27). Our numerical calculation is carried out as follows. The phase factor is taken as the axially symmetric form for the vortex core $\Phi = q^s \sum_i \phi_i$, $\alpha = q^{sp} \sum_i \phi_i$, where ϕ_i is the azimuthal angle for the j -th vortex core. The geometry of the system and the layout of the vortices are same as the GL calculation shown in Fig. 1. We set the rotating speed to be $\Omega = \Omega_c$ where the two-SVs texture becomes energetically stable against the one-SV texture at the system size R . For example, when the system size $R = 100 \mu\text{m}$, the critical speed is found to be $\Omega_c = 7.5 \text{ rad/s}$ which is the feasible rotating speed on experiments using rotating cryostat in ISSP.³⁶⁾ The integral in the left hand sides of eq. (28) is carried out numerically, and the distance of the vortices is determined by minimizing the gradient energy. This distance is consistent with the calculation based on the full GL theory. Our model is so simple that it is sufficient for our purpose to estimate only the energy scale of advantage of the HQV.

As seen in Fig. 3, the HQV advantage is of an order of 10^{-32} normalized with $K|\Delta|^2 \rho_s / \rho_s^0$. By comparing Fig. 2 and Fig. 3, we find that the relative instability of the HQV originating from the strong coupling effect becomes comparable to the energetically advantage of the HQV when the FL correction is taken into account.

The strong coupling correction in the bulk 4th order terms decreases as the pressure lowers, and the FL effect becomes important as the temperature decreases. Hence, the HQV is energetically stable in lower pressure and temperature region. However, in order to carry out the quantitative calculation of the energetics, we need the GL formulation systematically including the strong-coupling bulk 4th order terms and the FL correction of the gradient terms in equal footing with the general form of the OPs. If we use the most general representation of the OPs, that is, the spin and orbital parts of OPs are not separated, it is impossible to introduce the FL correction by the phenomenological way used by Cross.⁴¹⁾ These quantitative calculations of the stability remain as a future problem.

As shown above, the HQV has a single ZES bound at

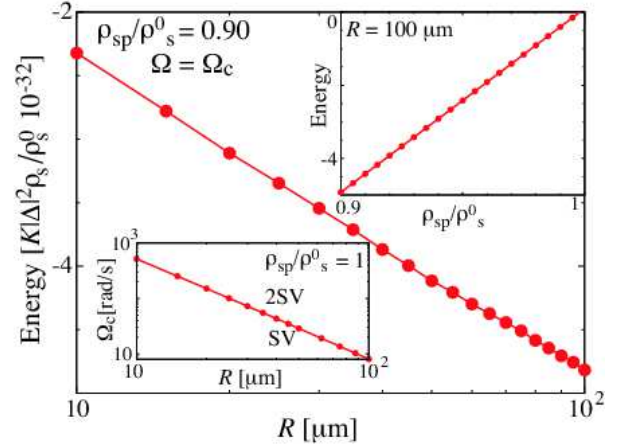


Fig. 3. (Color online) The main panel is the difference of the spatial variation energy f_{grad} normalized with $K|\Delta|^2 \rho_s / \rho_s^0$ as a function of the system size R where the FL correction is set to be $\rho_{sp}/\rho_s = 0.9$. The rotating speed is set to be $\Omega = \Omega_c$ where the two-SVs texture becomes stable compared with the one-SV texture for $\rho_{sp}/\rho_s = 1$. In our calculation, Ω_c is determined as a function of the system size shown in the bottom inset. The energetically stability of the HQV is proportional to $1 - \rho_{sp}/\rho_s$ as seen in the top inset.

the vortex core and obeys the non-Abelian statistics. On the other hand, SVs are energetically comparable with the HQV. Thus we consider the statistics of them in the following section.

4. Excitations and Braiding of Singular Vortex

As shown in the previous section, the stability of the HQV remains as a problem. Then, in this section, we consider the structure of the excitation and braiding of the SV. Especially, we notice the Zeeman effect due to an external field, and consider the following two situations: The magnetic fields applied perpendicular to the d -vectors and tilted from its direction.

4.1 \mathbf{H} perpendicular to d -vectors

The excitation composed of the self-Hermitian operators γ_{2j} and γ_{2j+1} describes the complex fermion eigenstate defined as

$$c_{2j} = (\gamma_{2j} + i\gamma_{2j+1})/\sqrt{2}. \quad (29)$$

The many-body ground state is described by the occupation number of the complex fermion. The complex fermion state can be understood as a spatially non-local state when the self-Hermitian excitations γ_{2j} and γ_{2j+1} are localized at spatially separated vortices. If the energy eigenvalue of the excitation is exactly zero, an adiabatic braiding of a vortex around another one changes the occupation number.⁷⁻⁹⁾ For instance, let us consider that there are four vortices V_i ($i = 1, 2, 3, 4$) and they have one Majorana quasiparticle γ_i at each vortex. We assume that the Majorana quasiparticles γ_1 and γ_2 (γ_3 and γ_4) form the complex fermion $c_{2(4)}$. If the vortex V_2 moves around V_3 , the operator of this braiding is described as^{7,8)}

$$\tau_{23} = (c_4^\dagger + c_4)(c_2^\dagger - c_2), \quad (30)$$

where we ignore the phase factor. This operator changes the occupation number of the complex fermion c_{2i} . This feature is known as the non-Abelian statistics of the vortices. When the odd number of the ZES appears at each vortex core, not less than one complex fermions are composed of the ZESs between different vortices. Then these vortices obey the non-Abelian statistics.

On the other hand, we consider the case where the number of ZESs localized at one vortex core is even. For instance, the ZESs are spin degenerate at the core of the well-isolated SV discussed in the previous section. This leads to the even number degeneracy of the self-Hermitian operators, γ_i^\uparrow and γ_i^\downarrow , at the core of each SV V_i , arising from the spin $|\uparrow\uparrow\rangle$ and $|\downarrow\downarrow\rangle$ sectors. We consider that there are four vortices. One can find two possible ways to form the complex fermion. (i) The self-Hermitian operators at the same vortex can make the complex fermion described as

$$a_i = (\gamma_i^\uparrow + i\gamma_i^\downarrow)/\sqrt{2}. \quad (31)$$

In this case, an exchange of the vortex means the exchange of the complex Dirac fermion a_i , implying that the braiding operator gets the only phase factor -1 and belongs to the Abelian group. (ii) The self-Hermitian operators at the spatially different vortices make the complex fermion described as

$$b_{2i}^\sigma = (\gamma_{2i}^\sigma + i\gamma_{2i+1}^\sigma)/\sqrt{2}. \quad (32)$$

In this case, if the vortex V_2 moves around V_3 , the braiding operator is described as

$$\begin{aligned} \tau_{23} = & (\{b_4^\uparrow\}^\dagger + b_4^\uparrow)(\{b_2^\uparrow\}^\dagger - b_2^\uparrow) \\ & \times (\{b_4^\downarrow\}^\dagger + b_4^\downarrow)(\{b_2^\downarrow\}^\dagger + b_2^\downarrow). \end{aligned} \quad (33)$$

When this transformation operates the quasiparticle vacuum state, the four complex fermions b_2^\uparrow , b_2^\downarrow , b_4^\uparrow , and b_4^\downarrow are created. Although the realization of b_{2i}^σ is not protected topologically, the braiding operator can change the occupation of the complex fermion and the vortices obey the non-Abelian statistics.

The situation where the ZESs are exactly degenerate can have both the ways to form the complex fermions a_i and b_{2i}^σ . However, the degeneracy of the ZES is removed by the finite distance of the vortices through the quasiparticle tunneling. We find that the complex fermion state is constructed from the ZESs belonging to the different vortices in one of the spin sectors when the external field is oriented exactly perpendicular to the direction of the d -vectors as shown in this section. We will show that the self-Hermitian particle belonging to a spin state does not hybridize with the counterpart in the different spin sectors. Therefore, the braiding of the vortices changes occupation number of the complex fermion in each spin sector and the braiding operator is approximately non-Abelian.

Under the assumption that the external field \mathbf{H} is applied to the direction perpendicular to the d -vector, we can block-diagonalize the BdG equation eq. (11) into the

two spin sectors $|\uparrow\uparrow\rangle$ and $|\downarrow\downarrow\rangle$ as

$$\int d\mathbf{r}_2 \begin{bmatrix} \hat{\mathcal{K}}_{\uparrow\uparrow}(\mathbf{r}_1, \mathbf{r}_2) & 0 \\ 0 & \hat{\mathcal{K}}_{\downarrow\downarrow}(\mathbf{r}_1, \mathbf{r}_2) \end{bmatrix} \underline{\mathcal{U}}\mathbf{u}_\nu(\mathbf{r}_2) = E_\nu \underline{\mathcal{U}}\mathbf{u}_\nu(\mathbf{r}_1), \quad (34)$$

where,

$$\hat{\mathcal{K}}_{\sigma\sigma} = \begin{bmatrix} H_0^\sigma(\mathbf{r}_1, \mathbf{r}_2) & \Delta_{\sigma\sigma}(\mathbf{r}_1, \mathbf{r}_2) \\ -\Delta_{\sigma\sigma}^*(\mathbf{r}_1, \mathbf{r}_2) & -H_0^{\sigma*}(\mathbf{r}_1, \mathbf{r}_2) \end{bmatrix}, \quad (35)$$

$$\underline{\mathcal{U}}\mathbf{u}_\nu(\mathbf{r}) = [u_\nu^\uparrow, v_\nu^\uparrow, u_\nu^\downarrow, v_\nu^\downarrow]^T, \quad (36)$$

where $\underline{\mathcal{U}}$ is an appropriate 4×4 unitary matrix and the spin quantization axis is set to be the direction parallel to \mathbf{H} . Notice that eq. (35) is equivalent to the Hamiltonian density of spinless p -wave superfluids and the components of the wave function belonging to $|\uparrow\uparrow\rangle$ ($|\downarrow\downarrow\rangle$) are given as $(u^{\uparrow(\downarrow)}, v^{\uparrow(\downarrow)})$. In the case of the SV, the two ZESs appear in two spin sectors, namely, $|\uparrow\uparrow\rangle$ and $|\downarrow\downarrow\rangle$. We consider systems with a plural number of the SV. When the vortex distance D_v is infinite, the ZES originating from each sector degenerates precisely. Any linear combination of these two states can be the eigenstate of the system. However, for finite D_v , this degeneracy of ZESs can be removed by the following two factors. One of them is the Zeeman effect for the energy splitting due to the quasiparticle tunneling and another is the splitting of the coherence length of two spin components under the strong external field.

First, we discuss the former factor. In a spinless p -wave superfluid, two ZESs bound in the neighboring vortices tunnel and interfere with each other. Then the energy of the complex fermions constructed in inter-vortex lifts from zero so that they are not exactly ZESs.^{49, 54} This energy shift oscillates and decreases exponentially as D_v becomes large, originating from quantum oscillation and localization of the wave function of the ZES.

We apply them into the spinful case. When we take account of the Zeeman effect, the chemical potentials of the up-spin and down-spin particles effectively shift as $\mu \pm \mu_n H$, where μ_n is the magnetic moment of the particle. The energy shift of ZESs in the spin $|\uparrow\uparrow\rangle$ and $|\downarrow\downarrow\rangle$ sectors can be calculated separately as,

$$\begin{aligned} E_\sigma \simeq & -\frac{2|A_{\sigma\sigma,-1}^0|}{\pi^{3/2}} \left[\frac{\cos(k_0 D_v + \pi/4)}{\sqrt{k_0 D_v}} \right. \\ & \left. \pm \frac{\mu_n H}{\epsilon_F} \frac{k_F}{k_0} \sqrt{D_v k_0} \sin(D_v k_0 + \pi/4) \right. \\ & \left. + \mathcal{O}\left(\frac{\mu_n H}{\epsilon_F}\right)^2 \right] \exp\left(-\frac{D_v}{\xi_{\sigma\sigma}}\right), \end{aligned} \quad (37)$$

where $k_0 = 2M\mu - \xi_{\sigma\sigma}^{-2}$. Because of the second term in this expression E_σ , the eigenvalues of the spin $|\uparrow\uparrow\rangle$ sector and the $|\downarrow\downarrow\rangle$ sector deviate from each other, and they can not hybridize with each other. Thus the complex fermions should be constructed between the vortices in each spin sector.

In order to demonstrate this, we numerically diagonalize the spinful BdG equation (11). This diagonalization is carried out in the two dimensional system under the

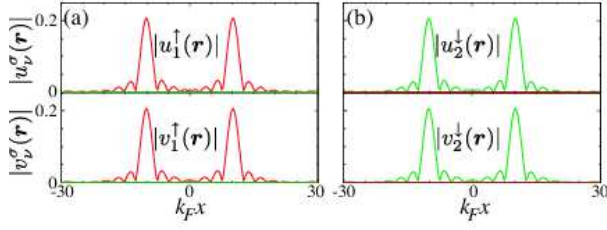


Fig. 4. (Color online) Cross sections of the amplitude of the wave functions u_1^\uparrow , v_1^\uparrow , u_2^\downarrow , and v_2^\downarrow at $y = 0$. We set the system size $k_F R = 30$, Zeeman splitting $\mu_n H/\epsilon_F = 10^{-4}$, the coherence length of the spin $|\sigma\sigma\rangle$ component $k_F \xi_{\sigma\sigma} = 2.5$, and the distance of the vortices $k_F D_v = 20$. The panel in (a) shows the wave function of the lowest energy excitation with $E_1/\epsilon_F = 2.08 \times 10^{-4}$ and the panel in (b) shows that of the second lowest energy excitation with $E_2/\epsilon_F = 2.09 \times 10^{-4}$.

OP given in eqs.(8) and (14). The geometry of the system is circle and the superfluid is confined by the rigid wall potential same as in the GL calculation. Here, we set $|A_{\sigma\sigma,-1}^0| \geq 0.1\epsilon_F$ in eq. (14) in order to secure the discreteness of the eigenvalue within the accuracy of calculation. Here, we consider two vortices, which are located at $(x, y) = (-D_v/2, 0)$ and $(D_v/2, 0)$. Although this calculation is carried out in the strong coupling region in the sense of $|A_{\sigma\sigma,-1}^0| \sim \epsilon_F$, the features of ZESs are independent of the details of the Hamiltonian. Therefore, the result from this calculation can be qualitatively applied to the weak coupling superfluid such as ^3He .

In Fig. 4, we show the wave function of the first and second lowest excitations in the presence of Zeeman splitting $\mu_n H/\epsilon_F = 1.0 \times 10^{-4}$ at the distance of the vortices $k_F D_v = 20$. These excitations are the complex fermion state as a consequence of the tunneling of the ZES bound at the vortex cores. Then near the vortex core, the self-Hermitian relation $u_\nu^\sigma = \{v_\nu^\sigma\}^*$ appears approximately. Furthermore, as shown in Fig. 4, these excitations are approximately composed of only one spin component of u_ν^σ and v_ν^σ . The u_2^\downarrow and v_2^\downarrow components of the first lowest excitation are of an order 10^{-7} of the component u_1^\uparrow and v_1^\uparrow . This means that the eigenstates originating from the $|\uparrow\uparrow\rangle$ and $|\downarrow\downarrow\rangle$ sectors are well-separated. We present in Fig. 5 the lowest eigenenergies, which oscillate and decay exponentially as a function of D_v . In Fig. 5, the difference of the eigenvalues between two different spin sectors is found to be about 10^{-2} times larger than the amplitude of eigenvalues E_σ , and to have the phase difference $\pi/2$ from the eigenvalue oscillation as shown in eq. (37). In realistic cases, since the amplitude of the OP is much smaller than the Fermi energy and the distance of the vortex is larger than this numerical simulation, these separations of the eigenvalue are quite small but finite. Therefore, even in a realistic situation, we conclude that the complex fermions can be constructed approximately by Majorana ZESs between different vortices in each spin sector.

In the case of spinful chiral p -wave superfluids under the strong external field, the amplitude and the coherence length of the OP component of the spin $|\uparrow\uparrow\rangle$ pair are not equal to those of the $|\downarrow\downarrow\rangle$ pair. In the language

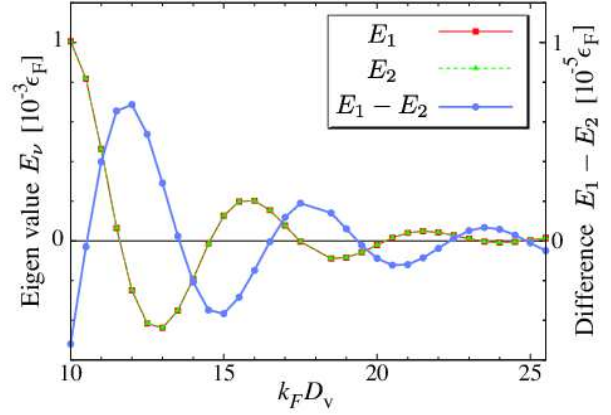


Fig. 5. (Color online) Lowest eigenenergies E_1 and E_2 originating from the spin $|\uparrow\uparrow\rangle$ and $|\downarrow\downarrow\rangle$ sectors and the difference $E_1 - E_2$ as a function of the distance of vortices. Here, we set the system size $k_F R = 30$, Zeeman splitting $\mu_n H/\epsilon_F = 10^{-4}$, the coherence length of the spin $|\sigma\sigma\rangle$ component $k_F \xi_{\sigma\sigma} = 2.5$. The left and right axes indicate the scale of the eigenenergies E_σ and the difference $E_1 - E_2$ respectively.

of ^3He , this situation is called the A_2 -phase. The coherence length $\xi_{\sigma\sigma}$ of the dominant spin component becomes smaller than that of the minor component and the ZES is tightly bound at the vortex core. The interference through the tunneling, shown in eq. (37), is weak for the major component and strong for the minor one. Therefore, the energy difference between the ZESs of each spin sector is enhanced by the deviation of $\xi_{\uparrow\uparrow}$ from $\xi_{\downarrow\downarrow}$. The eigenvalue in the dominant spin sector is closer to zero than that in the minor one. Thus, the eigenstate in the former has the Majorana character more precisely in the sense that the excitation of the complex fermion state is degenerate with the vacuum state. The excitation spectrum approaches continuously to that of the spinless case as this imbalance of OPs increases.

We numerically diagonalize the BdG equation for the OP given as

$$|A_{\uparrow\uparrow,-1}^0| = \frac{|\Delta_A|}{\sqrt{2}}(1 + X), \quad (38)$$

$$|A_{\downarrow\downarrow,-1}^0| = \frac{|\Delta_A|}{\sqrt{2}}(1 - X).$$

In a realistic system, the splitting $X \in [-1, 1]$ is proportional to the external field.⁵⁵⁾ In Fig. 6, we show the behavior of the energy splitting as a function of the imbalance of the OP. The solid lines are the energy of the eigenstate in the $|\downarrow\downarrow\rangle$ sector E_2 and the dashed lines are that of the spin $|\uparrow\uparrow\rangle$ sector. In the region $X > 0$ ($X < 0$), the eigenvalue E_1 (E_2) in the spin $|\uparrow\uparrow\rangle$ ($|\downarrow\downarrow\rangle$) sector becomes larger and the other eigenvalues E_2 (E_1) becomes closer to zero so that the difference $E_1 - E_2$ is also enhanced. For instance, at the splitting rate $X = 0.48$, this difference is of an order of $10^{-3}\epsilon_F$. In addition, this energy splitting is more enhanced by the short distance of vortices as shown in Fig. 6. The component closer to the zero energy has the Majorana character more precisely because of the degeneracy with the vacuum state of the quasiparticle.

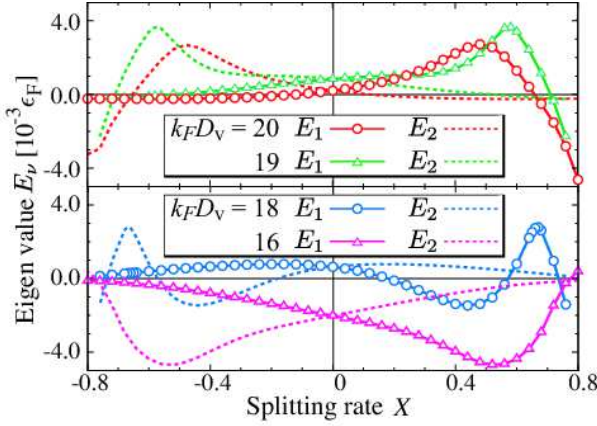


Fig. 6. (Color online) Lowest eigenenergies E_1 and E_2 originating from the spin $|\uparrow\uparrow\rangle$ (solid line) and $|\downarrow\downarrow\rangle$ (dashed line) sectors as a function of the splitting rate X defined in eq. (38), where we set $k_F R = 30$, $\mu_n H / \epsilon_F = 10^{-4}$, and $k_F D_v = 16, 18, 19$, and 20 . The energy differences of the eigenstate originating from two spin sectors (solid and broken line) are of an order of $10^{-6} \epsilon_F$ at the splitting rate $X = 0$. They are enhanced by increasing $|X|$ to the order of $10^{-3} \epsilon_F$.

It is unwelcome that the energy difference between the occupied state and the vacuum state of the complex fermion is finite. Because of the energy difference, the adiabatic exchange of vortices can not change the eigenstate of the complex fermions. Thus, we should carry out the braiding for the finite time scale $\epsilon_F / |A_{\sigma\sigma,-1}^0|^2 < t < (\epsilon_F)^{-1}$ where the lower boundary depends on the energy discreteness of the core bound states, $\Delta E \simeq |A_{\sigma\sigma,-1}^0|^2 / \epsilon_F$.¹⁷⁾ In the realistic value of ^3He , the time scale of $(\epsilon_F)^{-1}$ is almost infinite and $\epsilon_F / |A_{\sigma\sigma,-1}^0|^2$ is also much larger than the time scale of experiments. In the case of p -wave resonant Fermi gas^{11–13,15–17)} or the two dimensional polar fermionic molecules,^{56–58)} this range of the time scale could be feasible in experiments. Furthermore, since there is the energy difference of the many-body groundstate between the states before and after the braiding operation, the thermal relaxation changes the eigenstate transformed by the braiding.

4.2 \mathbf{H} tilted from $\mathbf{H} \perp d$ -vector

In the previous section, we assume that the d -vectors are perpendicular to the external field \mathbf{H} . However, it is difficult to align the d -vectors with this direction precisely in experiments. Then we consider the situation where the d -vectors are tilted to the direction perpendicular to \mathbf{H} .

Here, we also assume that the d -vectors are spatially uniform. Then we choose the directions of the d -vectors and the magnetization as $\hat{\mathbf{d}} = (1, 0, 0)$ and $\mathbf{H} = (H_x, 0, H_z)$, where one finds $A_{\uparrow\uparrow,m} = -A_{\downarrow\downarrow,m}$.

We first consider the eigenstate arising from an well-separated SV and regard the Zeeman effect arising from H_x as perturbation. In the unperturbed case, the BdG equation is block-diagonalized as shown in eq. (34), and the wave functions of the ZESs in these two sectors are

described as

$$\mathbf{u}_1(\mathbf{r}) = \left[u_1^\uparrow(\mathbf{r}), 0, \{u_1^\uparrow(\mathbf{r})\}^*, 0 \right]^T, \quad (39)$$

$$\mathbf{u}_2(\mathbf{r}) = \left[0, u_2^\downarrow(\mathbf{r}), 0, \{u_2^\downarrow(\mathbf{r})\}^* \right]^T, \quad (40)$$

$$u_\nu^\sigma(\mathbf{r}) = \exp(i\Phi_\sigma) \mathcal{N} J_0(k_0^\sigma r) \exp(-r/\xi_{\sigma\sigma}). \quad (41)$$

Here, Φ_σ is the phase of OP $A_{\sigma\sigma,-1}$ at the vortex core which arises from the phase of the other vortices, $J_0(x)$ is the Bessel function, \mathcal{N} is the normalization constant, and $k_0^\sigma = \sqrt{k_F^2 + \xi_{\sigma\sigma}^{-2} + \text{sgn}(\sigma)\mu_n H_z / \epsilon_F}$. Note that $k_0^\sigma \simeq k_F$ for $k_F \xi_{\sigma\sigma} \gg 1$ and $\mu_n H_z \ll \epsilon_F$, and the phase factor $\Phi_\uparrow - \Phi_\downarrow = \pi$ since $A_{\uparrow\uparrow,m} = -A_{\downarrow\downarrow,m}$. According to the ordinary perturbation theory, the perturbation H_x removes degeneracy as

$$\begin{aligned} \mathbf{u}'_1 &= \frac{1}{\sqrt{2}}(\mathbf{u}_1 + i\mathbf{u}_2) + \mathcal{O}(\mu_n H_x / \epsilon_F), \\ \mathbf{u}'_2 &= \frac{1}{\sqrt{2}}(\mathbf{u}_1 - i\mathbf{u}_2) + \mathcal{O}(\mu_n H_x / \epsilon_F). \end{aligned} \quad (42)$$

This wave function means that the operator of the eigenstate under finite H_x is described by a_i in eq. (31). Therefore, the two ZESs originating from different spin sectors hybridize in the same vortex core so that the hybridized state behaves as the Dirac fermion. As shown in the previous section, the vortices that have such a structure of the excitation can not involve the non-Abelian transformation of the many-body ground state by the braiding of the vortices.

The first order energy shift due to perturbation is estimated as

$$\begin{aligned} \Delta E^{(1)} &= \int d\mathbf{r} [\mathbf{u}'_1(\mathbf{r})]^\dagger \mu_n H_x \underline{\sigma}_x \mathbf{u}'_1(\mathbf{r}) \\ &\sim 4\mu_n H_x \xi_{\sigma\sigma} k_F, \end{aligned} \quad (43)$$

where the 4×4 Pauli matrix $\underline{\sigma}_i = \text{diag}[\hat{\sigma}_i, -\hat{\sigma}_i]$. Here, we use the asymptotic form of the Bessel function $J_0(x) \simeq \sqrt{2/(\pi x)} \cos(x - \pi/4)$ and assume that $(\xi_{\sigma\sigma} k_F)^{-1} \ll 1$ and $\xi_{\sigma\sigma}(k_0^\uparrow - k_0^\downarrow) \simeq \xi_{\sigma\sigma} k_F \mu_n H_z / \epsilon_F \ll 1$ by using the physical parameters for ^3He . In the case of the SV in ^3He in the parallel plate geometry which is defined in Fig. 7(a), the angle of d -vectors is determined as

$$\theta_d = \frac{1}{2} \tan^{-1} \left[\frac{\sin 2\theta_H}{(H_d/H)^2 - \cos 2\theta_H} \right], \quad (44)$$

where θ_d and θ_H is defined in Fig. 7(a). Equation (44) is derived by minimizing the dipole energy in eq. (21) and the magnetic interaction energy in eq. (22) within the London approximation, where $A_{+1}(\mathbf{r}) = |\Delta_A| \exp[i\Phi(\mathbf{r})]$, $A_{-1}(\mathbf{r}) = 0$, and the d -vectors are assumed as the unit vector. The resulting angle $\theta_d - \theta_H$ becomes maximum at $\theta_H = \pi/4$, as shown in Fig. 7(b). For instance, using $\theta_d = \pi/4$ and $H = 27$ mT, we estimate $H_x = 7.40 \times 10^{-2}$ mT. Then, we find $\Delta E^{(1)} = 1.68 \times 10^{-8} \epsilon_F$, which implies that the shift is much smaller than the gap $|\Delta_{\sigma\sigma}| \sim 10^{-3} \epsilon_F$ in ^3He . However, the symmetry separating two spin sectors is broken by this perturbation and the complex fermion a_i in eq. (31) is constructed in the same vortex core even for an in-

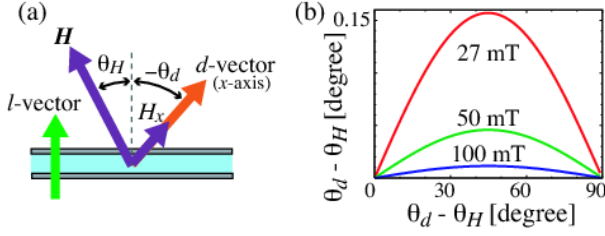


Fig. 7. (Color online) (a) A schematic diagram of the parallel plate geometry and the definition of θ_H , θ_d , and H_x . (b) The angle between the d -vector and the external field \mathbf{H} as a function of θ_H calculated in eq. (44) under the absolute value of the external field $H = 27, 50$, and 100 mT.

finitesimal field.

Whereas the perturbation H_x hybridizes the excitations in spin sectors, the interference through the tunneling of the quasiparticle separates the spin sectors shown in the previous section. In order to clarify this conflation, we diagonalize the BdG equation (11) where $\theta_d - \theta_H \neq \pi/2$. In Fig. 8(a), we plot the maximum amplitude of the wave function $|u_1^\uparrow(\mathbf{r})|$ and $|u_1^\downarrow(\mathbf{r})|$ of the lowest energy eigenstate as a function of $\theta_d - \theta_H$. As shown in previous section, the component $|u_1^\uparrow(\mathbf{r})|$ is finite and $u_1^\downarrow(\mathbf{r}) = 0$ at $\theta_d - \theta_H = \pi/2$, implying that this eigenstate originates from the spin $|\uparrow\uparrow\rangle$ sector. As seen in Fig. 8(a), when $\theta_d - \theta_H$ deviates from $\pi/2$, the minor component $|u_1^\downarrow(\mathbf{r})|$ grows rapidly, implying that the two sectors hybridize with each other. In fact, in the case of the coherence length $k_F \xi_{\sigma\sigma} = 1.5$, the two components of the wave functions become the equal order at $\theta_d - \theta_H = (89/180)\pi$: $|u_1^\uparrow(\mathbf{r})| \simeq |u_1^\downarrow(\mathbf{r})|$. This is consistent with eq. (42). We carry out the calculation under various $\mu_n H$ and $k_F \xi_{\sigma\sigma}$. Then, we find that the magnitude of the Zeeman shift $\mu_n H$ does not change the behavior of the hybridization. As shown in Fig. 8(a), the hybridization for tilting $\theta_d - \theta_H$ weakens with increasing the coherence length $k_F \xi_{\sigma\sigma}$. These results imply that the energy splitting at $\theta_d - \theta_H = \pi/2$ normalized with the amplitude of Zeeman splitting $|E_1 - E_2|/(\mu_n H)$ determines the rapidness of the hybridization. In order to quantify this, we define the initial slope of the hybridization for the \uparrow (\downarrow)-dominant mode described as

$$S_{\uparrow(\downarrow)}^u = \frac{d}{d(\theta_d - \theta_H)} \left(\frac{|u_{\text{Max}}^{\downarrow(\uparrow)}|}{|u_{\text{Max}}^{\uparrow(\downarrow)}|} \right) \quad (45)$$

$$S_{\uparrow(\downarrow)}^v = \frac{d}{d(\theta_d - \theta_H)} \left(\frac{|v_{\text{Max}}^{\downarrow(\uparrow)}|}{|v_{\text{Max}}^{\uparrow(\downarrow)}|} \right)$$

where $|u_{\text{Max}}^\sigma|$ and $|v_{\text{Max}}^\sigma|$ are the maximum value of the lowest energy wave functions $|u_1^\sigma(\mathbf{r})|$ and $|v_1^\sigma(\mathbf{r})|$. In Fig. 8(b), we plot the initial slope at the $\theta_d - \theta_H = \pi/2$ as a function of $|E_1 - E_2|/(\mu_n H)$. As shown in Fig. 8(b), all the results under different external fields, and layouts of vortices (one-SV and two-SV case) are on the same function, so that we ensure that the initial slope of the hybridization depends only on this ratio and yields a power law behavior in the region $|E_1 - E_2|/(\mu_n H) \leq 10^{-1}$.

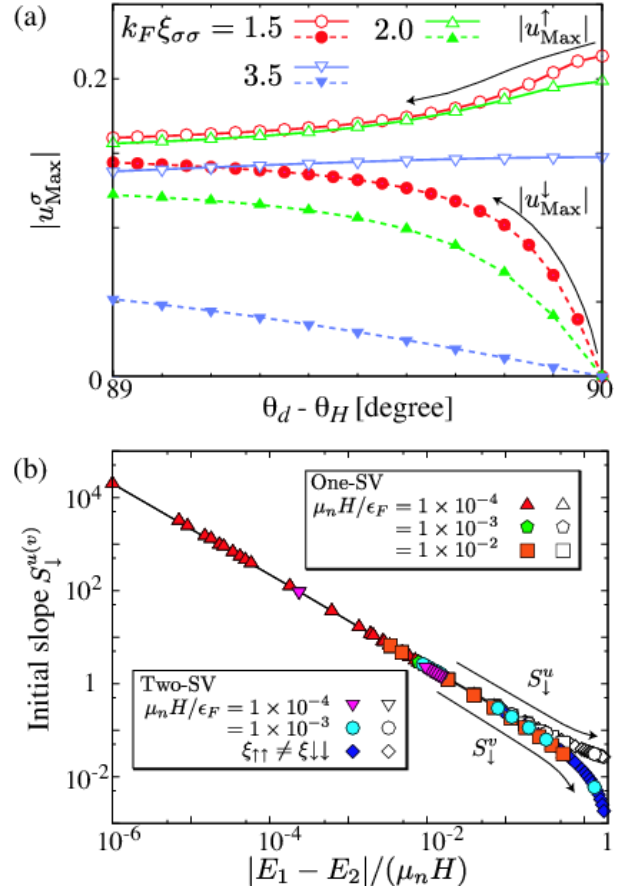


Fig. 8. (Color online) (a) The maximum value of the amplitude $|u_{\text{Max}}^\sigma|$ of the wave functions $u_1^\sigma(\mathbf{r})$ as a function of the angle between the d -vector and the magnetic field. The dashed line is $|u_{\text{Max}}^\downarrow|$ and the solid line is $|u_{\text{Max}}^\uparrow|$. (b) The absolute value of the initial slopes S_{\uparrow}^u and S_{\downarrow}^u of the hybridization of the minor spin components $|u_1^\uparrow|$ (open symbol) and $|v_1^\uparrow|$ (filled symbol), which is defined in eq. (45), as a function of $|E_1 - E_2|/(\mu_n H)$.

In addition, as shown in the previous section, the splitting of the coherence length, $\xi_{\uparrow\uparrow} \neq \xi_{\downarrow\downarrow}$, involves the enhancement of the energy difference of the ZESs. The initial slope becomes smaller due to this splitting and the result is present in Fig. 8(b) in the small splitting region $|E_1 - E_2|/(\mu_n H) \leq 1$ corresponding to $X \leq 10^{-2}$. With increasing $|X|$ corresponding to $|E_1 - E_2|/(\mu_n H) \geq 1$, the initial slope $S_{\sigma}^{u(v)}$ deviates from the line in Fig. 8(b) because the initial slope in eq. (45) is not a proper indicator of the behavior of the hybridization. That is due to the spatial expansion of the wave function in minor spin sector. However, for this region, $|E_1 - E_2|/(\mu_n H) > 1$ we find $S_{\sigma} \leq 10^{-1}$. Thus we can control the d -vectors to be perpendicular to the magnetic field enough to ignore the hybridization.

One can find that the accuracy on the direction of the magnetic field and weak coupling of minor component of the pair potentials $A_{\uparrow\uparrow,m}$ or $A_{\downarrow\downarrow,m}$ are required by the hybridization of two spin sectors. For example, for ^3He using the rotating cryostat under high external field,³⁶⁾ the feasible rotating speed is $\Omega \sim 10$ rad/s, the vortex distance is $D_v = 50 \mu\text{m}$, and the magnetic field is $H = 10$ T. In this situation, with the tilting angle of the external

field $\theta_H \sim 0.10$ degree, we estimate $\theta_d - \theta_H = 10^{-9}$ degree. It is concluded that even if the coherence length of the minor component of the OP is $\xi_{\sigma\sigma} k_F \geq 10^4$, we control the hybridization within $|u_1^\uparrow(r)|/|u_1^\downarrow(r)| \sim 10^{-2}$.

5. Summary and Conclusion

We have studied vortices and low energy excitations of the spinful chiral p -wave superfluid based on both the phenomenological Ginzburg-Landau (GL) theory and the microscopic Bogoliubov-de Gennes theory. We focus on the $^3\text{He-A}$ phase between parallel plates under a magnetic field.

In spinful chiral superfluids, possible candidates of the vortex texture are the singular vortex (SV) and the half-quantum vortex (HQV). In §3, we discuss the energetics of these textures. The free energy of the HQV is decreased by the Fermi liquid (FL) correction.^{42–44} However, we find that the strong coupling correction due to the spin fluctuations affects the energetics of the vortex texture at the vortex core and makes the HQV unstable compared with the SV as a result of our full GL calculation, which is not included in the discussion on refs. 42, 43, and 44. We calculate the contributions of the FL effect using London limit and of the strong coupling effect using full GL framework separately. It is demonstrated that the latter factor is comparable with the former under the rotation speed, a few rad/s, and near the transition temperature T_c , which is capable for the experiment of ^3He using rotating cryostat in ISSP. The quantitative calculation taking account of two factors described above is not established and remains as a future problem.

In §4, we have investigated the low energy excitations and the statistics of the SV. It is well-known that the HQV has the Majorana quasiparticle zero energy states (ZES), which are topologically protected. In SVs, the spin $|\uparrow\uparrow\rangle$ and $|\downarrow\downarrow\rangle$ components of the order parameter (OP) have the singularity at the same position so that the SV texture has the two zero energy excitations localized at the vortex cores. These behavior changes as the angle between the d -vectors and the external field \mathbf{H} varies.

In §4.1, we have considered the case where the d -vectors are exactly perpendicular to \mathbf{H} . In the case of ^3He between parallel plates, this situation is realized by applying the sufficiently strong external field and its direction perpendicular to the plates enough accurately. In this situation, the SV has the degenerate two ZESs which originate from the spin $|\uparrow\uparrow\rangle$ and $|\downarrow\downarrow\rangle$ sectors when the vortex distance is infinite. This leads to the Abelian statistics of vortices. However, for the finite vortex distance, the ZESs split through interference of their wave functions. Then, the degeneracy is removed and the spin $|\uparrow\uparrow\rangle$ and $|\downarrow\downarrow\rangle$ sectors can not hybridize with each other. Thus the excitation structures are found to be same as that of the spinless case and the SV approximately obeys the non-Abelian statistics. In addition, when the amplitudes of the OP components split under the high external field, that is, the coherence lengths of the spin $|\uparrow\uparrow\rangle$ pair is not identical to that of $|\downarrow\downarrow\rangle$ pair, the splitting of the eigenenergy is more enhanced by the interference of the zero-energy wave functions.

In §4.2, we consider the case where the d -vectors are

tilted from the direction perpendicular to \mathbf{H} . We find that when the d -vectors are tilted, the eigenstates originating from the spin $|\uparrow\uparrow\rangle$ and $|\downarrow\downarrow\rangle$ sectors hybridize intensely and form the complex fermions in the one of the vortex cores. Then our numerical calculation demonstrates that the intensity of the hybridization is determined by the energy splitting of the eigenstates of two spin sectors when d -vector $\perp \mathbf{H}$. In order to control this hybridization in experiments, we have to carry out the experiment near the spin polarized state called the A_2 -phase.

Finally, in the case of ^3He , we have discussed that the statistics of the vortices in spinful chiral p -wave superfluids with the vortex distance D_v depends on external parameters as follows. In the low-temperature and low-pressure region, the HQV is stable, and the statistics of the vortices is non-Abelian. In the high-temperature and high-pressure region, the SV is stable as a consequence of the strong coupling effect. When the coherence length of either the spin $|\uparrow\uparrow\rangle$ or $|\downarrow\downarrow\rangle$ component of OPs is much smaller than an order of $10^{-1}D_v$, we can not control the hybridization of the spin sectors. Hence, it is found that the statistics of the SVs is Abelian. However, for the coherence lengths of larger than $10^{-1}D_v$, the statistics of the SVs is found to be non-Abelian.

Acknowledgments

The authors thank M. Ichioka and Y. Tsutsumi for helpful discussions. This work is supported by a grant of the Japan Society for the Promotion of Science.

- 1) A. J. Leggett: Rev. Mod. Phys. **47** (1975) 331.
- 2) M. M. Salomaa and G.E. Volovik: Rev. Mod. Phys. **59** (1987) 3533.
- 3) A. P. Mackenzie and Y. Maeno: Rev. Mod. Phys. **75** (2003) 657.
- 4) G. Moore and N. Read: Nucl. Phys. B **360** (1991) 362.
- 5) N. Read and D. Green: Phys. Rev. B **61** (2000) 10267.
- 6) *Ettore Majorana*, ed. by G. F. Bassani and the Council of the Italian Physical Society (Springer, Heidelberg, 2006).
- 7) D. A. Ivanov: Phys. Rev. Lett. **86** (2001) 268.
- 8) A. Stern, F. von Oppen, and E. Mariani: Phys. Rev. B **70** (2004) 205338.
- 9) M. Stone and S.-B. Chung: Phys. Rev. B **73** (2006) 014505.
- 10) C. Nayak, S. H. Simon, A. Stern, M. Freedman, and S. D. Sarma: Rev. Mod. Phys. **80** (2008) 1083.
- 11) V. Gurarie and L. Radzihovsky: Ann. Phys. **322** (2007) 2.
- 12) V. Gurarie and L. Radzihovsky: Phys. Rev. B **75** (2007) 212509.
- 13) T. Mizushima, M. Ichioka, and K. Machida: Phys. Rev. Lett. **101** (2008) 150409.
- 14) Y. Tsutsumi, T. Kawakami, T. Mizushima, M. Ichioka, and K. Machida: Phys. Rev. Lett. **101** (2008) 135302.
- 15) Y. Tsutsumi and K. Machida: J. Phys. Soc. Jpn. **79** (2010) 034301.
- 16) P. Massignan, A. Sanpera, and M. Lewenstein: Phys. Rev. A **81** (2010) 031607(R).
- 17) T. Mizushima and K. Machida: Phys. Rev. A **81** (2010) 053605.
- 18) M. Stone and R. Roy: Phys. Rev. B **69** (2004) 184511.
- 19) X. L. Qi, T. L. Hughes, S. Raghu, and S. C. Zhang: Phys. Rev. Lett. **102** (2009) 187001.
- 20) S.-B. Chung and S. C. Zhang: Phys. Rev. Lett. **103** (2009) 235301.
- 21) G. E. Volovik: JETP Lett. **90** (2009) 440.
- 22) Y. Nagato, S. Higashitani, and K. Nagai: J. Phys. Soc. Jpn. **78** (2009) 123603.

- 23) Y. Tsutsumi, T. Mizushima, M. Ichioka, and K. Machida: arXiv 1004.2122.
- 24) L. Fu and C. L. Kane: Phys. Rev. Lett. **100** (2008) 096407.
- 25) Y. Tanaka, T. Yokoyama, N. Nagaosa: Phys. Rev. Lett. **103** (2009) 107002
- 26) J. Linder, Y. Tanaka, T. Yokoyama, A. Sudbo, and N. Nagaosa: Phys. Rev. Lett. **104** (2010) 067001.
- 27) C. Chamon, R. Jackiw, Y. Nishida, S.-Y. Pi, L. Santos: Phys. Rev. B **81** (2010) 224515.
- 28) M. Sato, Y. Takahashi, and S. Fujimoto: Phys. Rev. Lett. **103** (2009) 020401.
- 29) S. Tewari, S. D. Sarma, and D.-H. Lee: Phys. Rev. Lett. **99** (2007) 037001.
- 30) N. B. Kopnin and M. M. Salomaa: Phys. Rev. B **44** (1991) 9667.
- 31) G. E. Volovik: *The Universe in a Helium Droplet*, (Clarendon Press, Oxford, 2003) Chap. 23, p 288.
- 32) T. Kawakami, Y. Tsutsumi, and K. Machida: J. Phys. Soc. Jpn **79** (2010) 044607.
- 33) D. Vollhardt and P. Wölfle: *The Superfluid phase of Helium 3* (Taylor and Francis, London, 1990).
- 34) J. C. Wheatley: Rev. Mod. Phys. **47** (1975) 415.
- 35) D. S. Greywall: Phys. Rev. B **33** (1986) 7520.
- 36) M. Yamashita, K. Izumina, A. Matsubara, Y. Sasaki, O. Ishikawa T. Takagi, M. Kubota, and T. Mizusaki: Phys. Rev. Lett. **101** (2008) 025302.
- 37) R. G. Bennett, L. V. Levitin, A. Casey, B. Cowan, J. Parpia and J. Saunders: J. Low Temp. Phys. **158** (2010) 163.
- 38) K. Kono: J. Low Temp. Phys. **158**, (2010) 288.
- 39) P. W. Anderson and W. F. Brinkman: Phys. Rev. Lett. **30** (1973) 1108.
- 40) G. E. Volovik and V. P. Mineev: JETP Lett. **24** (1976) 561.
- 41) M. C. Cross: J. Low Temp. Phys. **21** (1975) 525.
- 42) M. M. Salomaa and G. E. Volovik: Phys. Rev. Lett. **55** (1985) 1184.
- 43) S.-B. Chung, H. Bluhm, and E. A. Kim: Phys. Rev. Lett. **99** (2007) 197002.
- 44) V. Vakaryuk and A. J. Leggett: Phys. Rev. Lett. **103** (2009) 057003.
- 45) T. Kawakami, Y. Tsutsumi, and K. Machida: Phys. Rev. B **79** (2009) 092506.
- 46) J. C. Light, I. P. Hamilton, and J. V. Lill: J. Chem. Phys. **82** (1985) 1400.
- 47) D. Baye and P.-H. Heenen: J. Phys. A: Math. Gen. **19** (1986) 2041.
- 48) D. E. Manolopoulos and R. E. Wyatt, Chem. Phys. Lett. **152** (1988) 23.
- 49) T. Mizushima and K. Machida: Phys. Rev. A **82** (2010) 023624.
- 50) J. A. Sauls and J. W. Serene: Phys. Rev. B **24** (1981) 183.
- 51) A. L. Fetter: *Progress in Low Temperature Physics*, ed. by D. F. Brewer (Elsevier Science Publishers, Amsterdam, 1986) Vol. X, p. 1.
- 52) E. V. Thuneberg: J. Low Temp. Phys. **122** (2001) 657.
- 53) T. Kita: Phys. Rev. B **66** (2002) 224515.
- 54) M. Cheng, R. M. Lutchyn, V. Galitski, and S. D. Sarma: Phys. Rev. Lett. **103** (2009) 107001.
- 55) V. Ambegaokar and N. D. Mermin: Phys. Rev. Lett. **30** (1973) 81.
- 56) G. M. Bruun and E. Taylor: Phys. Rev. Lett. **101** (2008) 245301.
- 57) N. R. Cooper and G. V. Shlyapnikov: Phys. Rev. Lett. **103** (2010) 155302.
- 58) T. Shi, J.-N. Zhang, C.-P. Sun, and S. Yi: arXiv:0910.4051v1.